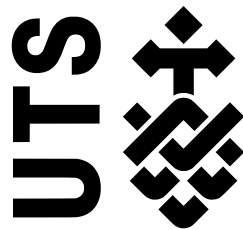


BrachyShade: Real-time Quality Assurance for High Dose Rate Brachytherapy

by

Roumani Alabd

A dissertation submitted in fulfilment of the requirements for the degree
Master of Engineering by Research



School of Electrical and Data Engineering
Faculty of Engineering and Information Technology
University of Technology Sydney

May 2018

Certificate of Original Authorship

I, Roumani Alabd, declare that this thesis titled, BrachyShade: Real-time Quality Assurance for High Dose Rate Brachytherapy, and the work presented in it is my own. I confirm that:

- This work was done wholly or mainly while in candidature for a research degree at this University.
- Where any part of this thesis has been previously submitted for a degree or any other qualification at this University or any other institution, this has been clearly stated.
- Where I have consulted the published work of others, this is always clearly attributed.
- Where I have quoted from the work of others, the source is always given. With the exception of such quotations, this thesis is entirely my own work.
- I have acknowledged all main sources of help.
- Where the thesis is based on work done by myself jointly with others, I have made clear exactly what was done by others and what I have contributed myself.

Production Note:
Signature removed
prior to publication.

May 2018
Roumani Alabd

Acknowledgements

I would first like to thank my thesis advisor Dr Daniel Franklin of the School of Electrical and Data Engineering at University of Technology Sydney. The door to Dr Franklin office was always open whenever I ran into a spot of troubles or had a question about my research or writing. He consistently allowed this paper to be my own work, but steered me in the right direction whenever he thought I needed it. This thesis would not be possible without his consistent and illuminating instructions.

I would also like to acknowledge Dave Hughes of the Climate Change Cluster (C3), Science Faculty at University of Technology Sydney as the second reader of a big portion of this thesis, and I am gratefully indebted to him for his very valuable comments on this work.

Finally, I must express my very profound gratitude to my parents and to my family for providing me with unfailing support and continuous encouragement throughout my years of study and through the process of researching and writing this thesis. This accomplishment would not have been possible without them. Thank you.

Dedication

To My Father

Abstract

High dose rate (HDR) brachytherapy is a popular form of radiotherapy in which radiation is delivered to the tumour via a small sealed radioactive source, which is moved through a sequence of positions in an array of catheters pre-implanted in the target area. Brachytherapy offers a key advantage over external beam radiotherapy, since the radiation dose is delivered directly to the diseased tissue while minimising the dose applied to healthy tissue in proximity to the target volume.

The accuracy of source placement is critical to the success of HDR brachytherapy. Deviations between the planned source position and the actual position achieved during treatment, due to anatomical changes (e.g. due to swelling or post-imaging tumour growth) or imperfect catheter placement, can harm healthy tissue or under-irradiate diseased tissue. Therefore, a reliable, accurate, real-time 3D source tracking system would be extremely valuable for treatment quality assurance and would allow a treatment plan to be modified in real time if positioning errors are detected.

HDR BrachyView is an in-body source tracking system designed to monitor the location of a HDR prostate brachytherapy source developed at the Centre of Medical Radiation Physics at the University of Wollongong, based on a tungsten pinhole camera with a silicon pixellated photon detector. Source position is estimated by back-projecting images of the source projected through the pinholes onto the imaging plane. Although HDR BrachyView has been shown to perform very well, it is challenging to manufacture, and suffers from a small systemic error in position estimation.

BrachyShade proposes to replace the tungsten collimator with a series of small spherical or spheroidal tungsten occluders embedded in a plastic shell, suspended over

the same pixellated detector (TimePix) used in the original HDR BrachyView. Instead of tracking bright projections of the source, the shadow of the source will be tracked, and by parametrically fitting an analytic model of the shadow map (where the model parameters are source position and intensity), the source position will be estimated. The proposed design significantly simplifies the manufacturing process, lowering the costs of manufacturing; it will also allow many more photons to arrive at the detector, enabling faster acquisition of a high quality position estimate. The achievable accuracy is comparable to HDR BrachyView, with a wider field of view achievable, depending on the specific configuration of tungsten occluders.

This Thesis presents a set of Monte Carlo simulations of the system, performed in Geant4. A sophisticated analytic model of the shadow map has been derived, and an algorithm developed which estimates the source position by minimising the error between the output of the analytic model and the detected photon map. A post-processing stage eliminates the effects of Compton scatter, which are otherwise mathematically challenging to include in the analytic model. Exhaustive test results proving the accuracy of the algorithm are presented. A second analytic method for estimating source position via a hierarchical pattern-matching strategy is also described, and preliminary results presented.

Keywords: Cancer, HDR Brachytherapy, Quality Assurance

Abbreviations

| | |
|------|---|
| AAPM | American Association of Physicists in Medicine |
| ABS | American Brachytherapy Society |
| ACIM | Australian Cancer Incidence and Mortality workbooks |
| AIHW | Australian Institute of health and Welfare |
| AJCC | American Joint Committee on Cancer |
| BSDF | Backscatter dose fraction |
| BT | Brachytherapy |
| CCD | Charge-coupled device |
| CIRS | Computerized Imaging Reference Systems |
| CMRP | Centre for Medical Radiation Physics |
| CoG | Geometrical centre |
| CoMi | Ideal centre of mass |
| CRT | Conformal radiation therapy |
| CTV | Clinical Target Volume |
| DHT | Dihydrotestosterone |
| DRE | Digital rectal examination |
| DSP | Direct source projection |
| DVH | Dose Volume Histogram |
| D90 | The Dose Delivered to at least 90% of The Target Volume |
| D80 | The Dose Delivered to at least 80% of The Target Volume |
| EBRT | External Beam Radiotherapy |
| ESP | Extensive source projection |

| | |
|--------|--|
| ESTRO | The European Society for Radiotherapy and Oncology |
| FOV | Field of View |
| HDR | High Dose Rate |
| IAEA | International Atomic Energy Agency |
| IEEE | Institute of Electrical and Electronics Engineers |
| IGRT | Image-guided radiation therapy |
| IMRT | Intensity modulated radiation therapy |
| ISUP | International Society of Urological Pathology |
| LDR | Low Dose Rate |
| LET | Linear energy transfer |
| MOSFET | Metal Oxide Semiconductor Field Effect |
| PBT | Prostate Brachytherapy |
| PCB | Printed Circuit Board |
| PDR | pulsed Dose Rate |
| PSD | Plastic Scintillation Detector |
| PTV | Planning Target Volume |
| OARs | Organs at Risks |
| QA | Quality Assurance |
| SD | Standard deviation |
| SBR | Signal to background ratio |
| SDD | Source to detector distance |
| SEM | Error of the sample mean |
| SNR | Signal to Noise Ratio |
| SSIM | Structural Similarity Index |
| SVD | Singular Value Decomposition |
| TLD | Thermoluminescent Dosimeters |
| ToA | Time of arrival mode |
| ToT | Time over threshold mode |
| TPS | Treatment Planning System |
| TRUS | Transrectal Ultrasound |
| V100 | The Percentage of the Prostate Receiving %100 of the prescribed Dose |
| WED | Water-equivalent depth |

Table of contents

| | |
|---|------------|
| Abstract | v |
| Abbreviations | vii |
| List of figures | xii |
| List of tables | xiv |
| 1 Introduction | 1 |
| 1.1 Prostate Brachytherapy and the Need for Real-Time Quality Assurance | 2 |
| 1.2 Objectives and Overview | 3 |
| 1.3 Summary of Contributions and Structure of this Thesis | 4 |
| 1.3.1 Summary of Contributions | 4 |
| 1.3.2 Thesis Structure | 5 |
| 2 Literature Review | 7 |
| 2.1 Brachytherapy | 8 |
| 2.1.1 High Dose Rate and Low Dose Rate Brachytherapy | 9 |
| 2.1.2 Low Dose Rate (LDR) Brachytherapy | 10 |
| 2.1.3 High Dose Rate (HDR) Brachytherapy | 10 |
| 2.1.3.1 Implantation Techniques | 11 |
| 2.1.3.2 Isotope Selection | 12 |
| 2.1.4 The Need for Real-Time QA in Brachytherapy | 12 |

| | | |
|----------|--|-----------|
| 2.1.5 | HDR Prostate Brachytherapy | 13 |
| 2.2 | Causes of Error in Source Positioning in HDR Prostate Brachytherapy | 13 |
| 2.3 | The Physics of Source Tracking | 16 |
| 2.3.1 | Photoelectric Effect | 18 |
| 2.3.2 | Compton Scattering | 18 |
| 2.3.3 | Attenuation of Radiation | 21 |
| 2.4 | A Survey of Nuclear Medical Imaging Systems | 22 |
| 2.4.1 | Computed Tomography (CT) | 22 |
| 2.4.2 | Ultrasound | 23 |
| 2.4.3 | Dosimeters and Source Tracking Methods in HDR Brachytherapy Treatment | 24 |
| 2.5 | HDR BrachyView | 30 |
| 2.5.1 | Pixellated Silicon Detector | 31 |
| 2.5.2 | Collimator | 33 |
| 2.5.3 | HDR BrachyView Source Localisation Algorithm | 34 |
| 2.5.4 | Limitations | 35 |
| 2.6 | Conclusion | 36 |
| 3 | Methodology | 38 |
| 3.1 | Probe Design | 39 |
| 3.2 | Source Position Estimation Algorithm | 41 |
| 3.3 | Analytic Model | 42 |
| 3.4 | Compton Scatter Correction | 45 |
| 3.5 | An Alternative Source Localisation Algorithm: Hierarchical Pattern Matching | 48 |
| 3.6 | Monte Carlo simulations | 50 |
| 3.6.1 | Simulation Framework, Models and Parameters | 50 |
| 3.6.2 | Source Model | 50 |
| 3.6.3 | Planned Simulations and Analysis | 51 |
| 3.6.3.1 | Compton Scatter Evaluation | 52 |
| 3.6.3.2 | Source Position Estimation Results Prior to Compton Scatter Correction | 52 |
| 3.6.3.3 | Results After Compton Scatter Correction | 52 |
| 3.6.4 | Fast Hierarchical Pattern Matching | 52 |
| 3.7 | Conclusion | 53 |

| | | |
|----------|--|-----------|
| 4 | Results and Discussion | 54 |
| 4.1 | Compton Scatter Evaluation and Analytic Model Validation | 54 |
| 4.2 | Uncorrected Position Estimation Results | 58 |
| 4.3 | Compton Scatter Correction | 58 |
| 4.3.1 | Results from probe design with 3 occluders; Restricted FoV . . . | 58 |
| 4.3.2 | 3 Occluder Probe with Extended FoV | 65 |
| 4.3.3 | 7 Occluder Probe with Extended FoV | 67 |
| 4.3.4 | Resource requirements and computational complexity | 68 |
| 4.4 | Fast Hierarchical Pattern Matching | 69 |
| 4.4.1 | Error evaluation at selected points | 69 |
| 4.4.2 | Resource requirements and computational complexity | 70 |
| 4.5 | Conclusions | 70 |
| 5 | Conclusions and Future Work | 72 |
| 5.1 | Conclusion | 72 |
| 5.2 | Future Work | 74 |
| | Bibliography | 75 |

List of figures

| | | |
|-----|--|----|
| 2.1 | Causes of catheter position shift relative to the prostate [33]. | 15 |
| 2.2 | Photons interacting with the human body experiencing three possible modes of interaction [38]. | 17 |
| 2.3 | Photoelectric absorption. The diagram shows a 100-keV photon undergoing photoelectric absorption during interaction with an iodine atom [39]. | 19 |
| 2.4 | Multiple interactions of a photon passing through matter. Energy is transferred to electrons in a sequence of photon-energy reducing interactions [12]. | 20 |
| 2.5 | Linear Attenuation Coefficient [38] | 20 |
| 2.6 | Mass attenuation coefficient [38] | 22 |
| 2.7 | Schematic diagram showing the HDR BrachyView probe relative to prostate phantom [27]. | 31 |
| 2.8 | The Timepix ASIC chip. The sensor chip is bump-bonded to the readout chip. Wire bonds are visible[75] | 32 |
| 2.9 | Multi-pinhole collimator hole spacing[26] | 34 |
| 3.1 | The BrachyShade probe with 3 occluders. | 39 |
| 3.2 | The BrachyShade probe with 7 occluders. | 40 |
| 3.3 | The simulated ^{192}Ir HDR brachytherapy source. The core consists of pure iridium with a uniform distribution of ^{192}Ir , surrounded by a steel shell [82, 83]. | 50 |

| | | |
|-----|--|----|
| 4.1 | Sensitivity as a function of depth for Monte Carlo simulations with and without the presence of a scattering medium, and for the analytic model, showing the most four significant source energies. | 56 |
| 4.2 | Example of raw output from Geant4 simulations (37×10^9 primary particles, real ^{192}Ir source model centred at (18.5, 20, 60) mm), with the results of the fitting process. Without Compton scatter correction, the fitting algorithm estimates the location as being (22.0, 21.9, 70.8) mm. | 57 |
| 4.3 | Comparison of simulation output and analytic model for source located at (2.5, 5, 20) mm. | 59 |
| 4.4 | Uncorrected error vector field for 3-occluder system as a function of estimated source position. | 60 |
| 4.5 | Compton-scatter error correction vector field for 3-occluder system, shown as a function of estimated source position. The field is a 3D second-order polynomial fitted to the raw error vector field. | 61 |
| 4.6 | Residual error after correction added to original position estimate. | 62 |
| 4.7 | Error as a function of distance from (0, 0, 0), before and after applying the Compton scatter correction field. | 63 |
| 4.8 | Error vector field for 3 occluders as a function of estimated source position; fitted second-order polynomial model of the error vector field; residual error after correction added to original position estimate for the whole FOV. | 66 |
| 4.9 | Error vector field for 7 occluders as a function of estimated source position; fitted second-order polynomial model of the error vector field; residual error after correction added to original position estimate. | 67 |

List of tables

| | | |
|-----|--|----|
| 3.1 | ¹⁹² Ir gamma spectrum [82] | 51 |
| 4.1 | Residual error prior to Compton scatter correction | 64 |
| 4.2 | Residual error after Compton scatter correction; with an accurate model of an HDR brachytherapy source, the residual error is less than 1.2941 mm for all evaluated source positions and less than 0.4141 mm in 75% of positions. This represents a reduction in the error by a factor of 2.4-5.2. | 64 |
| 4.3 | Residual error statistics after Compton scatter correction, 3-occluder probe, with all points used to fit the correction coefficients. | 66 |
| 4.4 | Residual error statistics after Compton scatter correction, 7-occluder probe, with all points used to fit the correction coefficients. | 68 |
| 4.5 | Residual error statistics after Compton scatter correction with fast hierarchical pattern-matching algorithm; probe is the 3-occluder variant, with all points used to fit the correction coefficients. | 70 |